Neuro-Oncology
26(4), 653–669, 2024 | https://doi.org/10.1093/neuonc/noad232 | Advance Access date 9 December 2023

Metabolic modulation of histone acetylation mediated by HMGCL activates the FOXM1/β-catenin pathway in glioblastoma

Yanfei Sun, Guangjing Mu, Xuehai Zhang, Yibo Wu, Shuai Wang, Xu Wang, Zhiwei Xue, Chuanwei Wang, Jilong Liu, Wenbo Li, Lin Zhang, Yunyun Guo, Feihu Zhao, Xuemeng Liu, Zhiyi Xue, Yan Zhang, Shilei Ni, Jian Wang, Xingang Li, Mingzhi Han, and Bin Huang

All author affiliations are listed at the end of the article

Corresponding Authors: Bin Huang, PhD, Department of Neurosurgery, Qilu Hospital, Cheeloo College of Medicine and Institute of Brain and Brain-Inspired Science, Shandong University; Jinan Microecological Biomedicine Shandong Laboratory and Shandong Key Laboratory of Brain Function Remodeling, Jinan, China (hb@sdu.edu.cn); Mingzhi Han, PhD, MD, Department of Neurosurgery, Qilu Hospital, Cheeloo College of Medicine and Institute of Brain and Brain-Inspired Science, Shandong University; Jinan Microecological Biomedicine Shandong Laboratory and Shandong Key Laboratory of Brain Function Remodeling, Jinan, China (mingzhi.han@sdu.edu.cn); Xingang Li, PhD, MD, Department of Neurosurgery, Qilu Hospital, Cheeloo College of Medicine and Institute of Brain and Brain-Inspired Science, Shandong University; Jinan Microecological Biomedicine Shandong Laboratory and Shandong Key Laboratory of Brain Function Remodeling, Jinan, China (lixg@sdu.edu.cn).

Abstract

Background. Altered branched-chain amino acid (BCAA) metabolism modulates epigenetic modification, such as H3K27ac in cancer, thus providing a link between metabolic reprogramming and epigenetic change, which are prominent hallmarks of glioblastoma multiforme (GBM). Here, we identified mitochondrial 3-hydroxymethyl-3-methylglutaryl-CoA lyase (HMGCL), an enzyme involved in leucine degradation, promoting GBM progression and glioma stem cell (GSC) maintenance.

Methods. In silico analysis was performed to identify specific molecules involved in multiple processes. Glioblastoma multiforme cells were infected with knockdown/overexpression lentiviral constructs of HMGCL to assess malignant performance in vitro and in an orthotopic xenograft model. RNA sequencing was used to identify potential downstream molecular targets.

Results. *HMGCL,* as a gene, increased in GBM and was associated with poor survival in patients. Knockdown of HMGCL suppressed proliferation and invasion in vitro and in vivo. Acetyl-CoA was decreased with HMGCL knockdown, which led to reduced NFAT1 nuclear accumulation and H3K27ac level. RNA sequencing-based transcriptomic profiling revealed *FOXM1* as a candidate downstream target, and HMGCL-mediated H3K27ac modification in the *FOXM1* promoter induced transcription of the gene. Loss of FOXM1 protein with HMGCL knockdown led to decreased nuclear translocation and thus activity of β-catenin, a known oncogene. Finally, JIB-04, a small molecule confirmed to bind to HMGCL, suppressed GBM tumorigenesis in vitro and in vivo.

Conclusions. Changes in acetyl-CoA levels induced by HMGCL altered H3K27ac modification, which triggers transcription of *FOXM1* and β-catenin nuclear translocation. Targeting HMGCL by JIB-04 inhibited tumor growth, indicating that mediators of BCAA metabolism may serve as molecular targets for effective GBM treatment.

Key Points

- HMGCL enhances H3K27ac modification by promoting acetyl-CoA production.
- Enhancing expression of *FOXM1* by HMGCL-mediated H3K27ac alteration promotes nuclear translocation of β-catenin.

Graphical Abstract

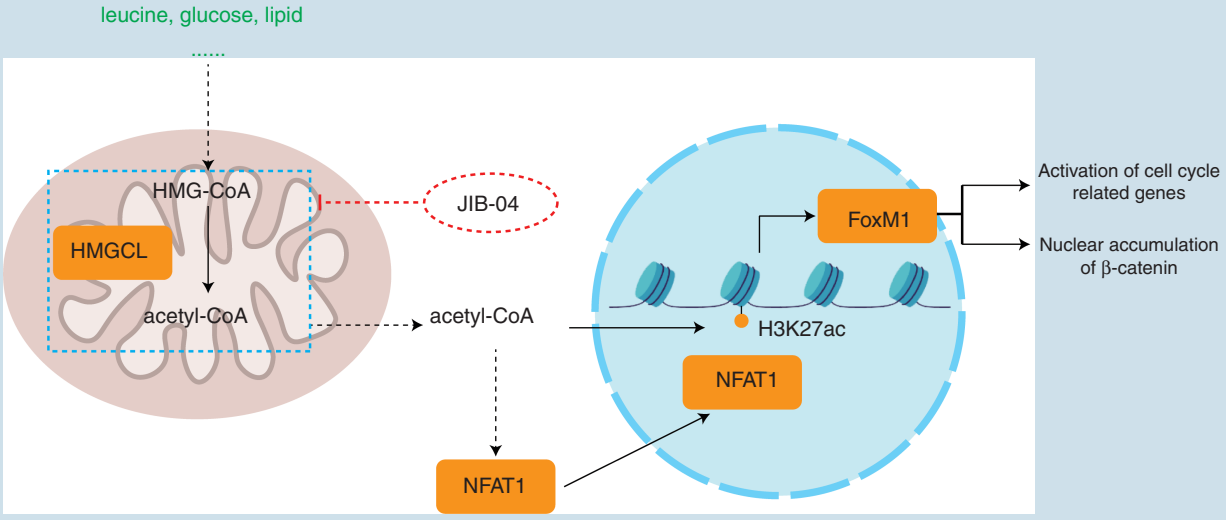

Importance of the Study

Deciphering the molecular basis of the crosstalk between metabolic reprogramming and epigenetic abnormalities may help to optimize treatment paradigms and establish new therapeutic options for glioblastoma multiforme (GBM). This study illustrates a crucial role for branched-chain amino acid (BCAA) metabolism in glioma stem cell performance and maintenance, and GBM progression. An enzyme involved in BCAA metabolism, mitochondrial 3-hydroxymethyl-3-methylglutaryl-CoA lyase (HMGCL), is overexpressed in GBM, and associated with poor survival in patients, and enhances H3K27ac modification. Enhanced H3K27ac modification mediated by HMGCL-induced metabolic changes promoted expression of an oncogene, *FOXM1*. Upregulation of *FOXM1* functioned as a transcription factor for the transcription of oncogenes and a binding partner causing nuclear translocation of β-catenin. Targeting HMGCL with the small-molecule inhibitor JIB-04 led to decreased tumor growth in an orthotopic tumor model, thus implicating the enzyme as a candidate molecule for the treatment of GBM.

Glioblastoma multiforme (GBM) is the most aggressive central nervous system (CNS) tumor.[1] Although rigorous multimodal treatment consisting of surgery, radiotherapy, and chemotherapy is the current standard of care, the prognosis of GBM patients has remained poor over decades.[2] Intratumoral heterogeneity as a result of tumor genetics, epigenetics, and microenvironmental interactions underlies GBM malignancy and treatment failure. Glioma stem cell (GSC) is regarded as the pinnacle of tumor-cellular hierarchy[3] and a major factor contributing to recurrence. Hallmarks of cancers, including deregulation of cellular metabolism and nonmutational epigenetic reprogramming, promote tumor heterogeneity and development of GSCs.[4] Novel therapeutic strategies with a comprehensive understanding of these characteristics of GBM are necessary to advance treatment of the disease.

Recently, due to the improvement of molecular pathology, glioma progression has been associated with different types of epigenetic phenomena, such as histone modifications.[5] Chromatin-regulating factors alter modification of locations and density of nucleosomes on chromosomes, and mediate posttranscriptional modification of histones or incorporation of histone variants within nucleosomes.[6,7] Special therapeutic strategies have been designed based on development of epigenetics, which provided a basis for novel approaches for GBM treatment.[5,7] For example, histone deacetylation inhibitors (HDACi), such as Vorinostat, have been introduced into clinical trials for GBM patients (NCT03426891, NCT03243461). Recent studies have established a linkage between metabolism and epigenetics, with products of metabolic pathways influencing epigenetics and gene transcription.[8,9] Nutritional supplements and metabolic conditions of tumor cells alter expression of genes, which is induced by communication between the nucleus, cytoplasm, and mitochondria.[10,11] For example, fluctuations in acetyl-CoA affect histone acetylation levels, which influence transcription of oncogenes in GBM.[12] With a better understanding of this regulatory model, we might modulate essential genes more precisely, thus providing new insights into treatment of glioma.

Recent studies have revealed the significance of altered branched-chain amino acid (BCAA) metabolism in various human cancers,[13,14] including GBM,[15] lung cancer,[16] and so on. BCAA (valine, leucine, and isoleucine) metabolism has been confirmed to affect epigenetic modification, such as H3K27ac[17] and m6A modification.[18] Multiple models have been developed to clarify the function of altered BCAA metabolism in tumor progression, stem cell maintenance, and drug resistance,[19] indicating that targeting BCAA metabolism is an attractive therapeutic approach for managing human cancers.

Mitochondrial 3-hydroxymethyl-3-methylglutaryl-CoA lyase (HMGCL) is a metabolic enzyme involved in the last step of leucine degradation.[20] HMGCL catalyzes conversion of 3-hydroxymethyl-3-methylglutaryl Coenzyme A (HMG-CoA) into acetyl-CoA and acetoacetate. Acetoacetate could be transformed into β-hydroxybutyrate (β-OHB) by 3-hydroxybutyrate dehydrogenase (BDH1). Upregulation of HMGCL-induced activation of MEK1/ERK1 axis by acetoacetate, thereby promoting the growth of *BRAF*-mutated melanoma.[21] β-OHB mediated by HMGCL could enhance malignancy of pancreatic cancer and inhibit growth of hepatocellular carcinoma.[22,23] However, function of HMGCL-mediated metabolism alteration in GBM and underlying molecular mechanisms have not yet been rigorously investigated.

In this study, we found BCAA degradation was essential for GSC maintenance and GBM progression, while HMGCL was overexpressed in GBM. We demonstrated that HMGCL promoted GSC maintenance and malignant performance of GBM through metabolic modification of H3K27ac, which induced transcription of oncogenes, such as the transcription factor *FOXM1*. These changes in HMGCL-mediated H3K27ac were caused by variations in intracellular acetyl-CoA concentrations. Furthermore, FOXM1 mediated nuclear accumulation of β-catenin, a critical component of WNT signaling. Finally, we showed that JIB-04, a small-molecule inhibitor, targeted HMGCL, and thus, provided a promising candidate molecule for the treatment of GBM.

Materials and Methods

Ethics Statement and Clinical Glioma Tumor Specimens

Approval for the protocols in the study was granted by the Ethics Committee of Qilu Hospital of Shandong University (Jinan, China; approval number: KYLL-2017(KS)-090). This study was conducted in full adherence to relevant regulations and guidelines. Human glioma tissue samples were obtained from surgeries performed on patients at Qilu Hospital. Non-neoplastic brain tissue samples were obtained from patients requiring surgery for traumatic brain injury events. All patients enrolled provided written informed consent.

Data Processing and Bioinformatics Analysis

Expression data and associated clinical data were downloaded from GlioVis (http://gliovis.bioinfo.cnio.es/). Transcriptome data of GSC and DGC, gene sets of metabolism processes and mDNAsi were obtained from article published.[24–26] Signatures of metabolism processes were based on single-sample gene set enrichment analysis (GSEA). Single-cell RNA-seq analysis was based on GSE131928.

Tumorsphere Formation Assays

GSCs (1000 cells/mL per well) were seeded in 6-well ultra-low adhesion plates (Corning Inc.) or general plates (Corning Inc.) and cultured for 10 days. Inverted phase-contrast microscopy (Nikon) was used to count and acquire images of the nonadherent tumorspheres.

Statistical Analysis

The relationship between gene expression and mDNAsi was determined using Pearson correlation analysis. Kaplan–Meier survival curves were generated and compared using the log-rank test. Paired or unpaired Student's *t* tests for 2-group comparisons and 1-way analysis of variance (ANOVA) for multigroup comparisons were performed using GraphPad Prism 8.0. Data for each group were represented as the mean standard error of the mean (SD/SEM) and *P* values < .05 were considered to be statistically significant.

See Supplementary Methods for additional details on all methods.

Results

BCAAs Are Essential for GSC Maintenance and GBM Progression

We performed comparative metabolomic analysis of 40 gene sets[25] in a public data set,[24] which revealed enrichment of pathways related to the degradation of BCAAs in GSCs compared with matched differentiated GBM cells (DGCs) (Figure 1A; Supplementary Table ST1). Since BCAA metabolism has been recognized as an alternative source of energy to drive proliferation, the resultant metabolites have been considered as factors regulating malignant progression.[19] Our results showed that valine, leucine, and isoleucine degradation signatures were higher in the classical molecular subtype of GBM (Figure 1B). Further analysis demonstrated that higher expression of these signatures was associated with specific genetic markers of higher-grade gliomas, including *EGFR* amplification (Figure 1C), wild-type *IDH1*, and non-codeleted 1p/19q (Figure 1D and E). These results demonstrated that increased expression of BCAA degradation pathways was associated with high-grade gliomas. In addition, high scores were also associated with poorer prognosis in GBM patients based on the Rembrandt and Gravendeel databases (Figure 1F). Taken together, BCAA metabolism emerged as a potential pathway promoting GSC maintenance and GBM progression.

HMGCL is Overexpressed in GBM With Poor Prognosis

To identify a specific molecular target for GBM in BCAA metabolism, we performed survival analysis (Threshold: $P < .001$) and multivariate Cox analysis

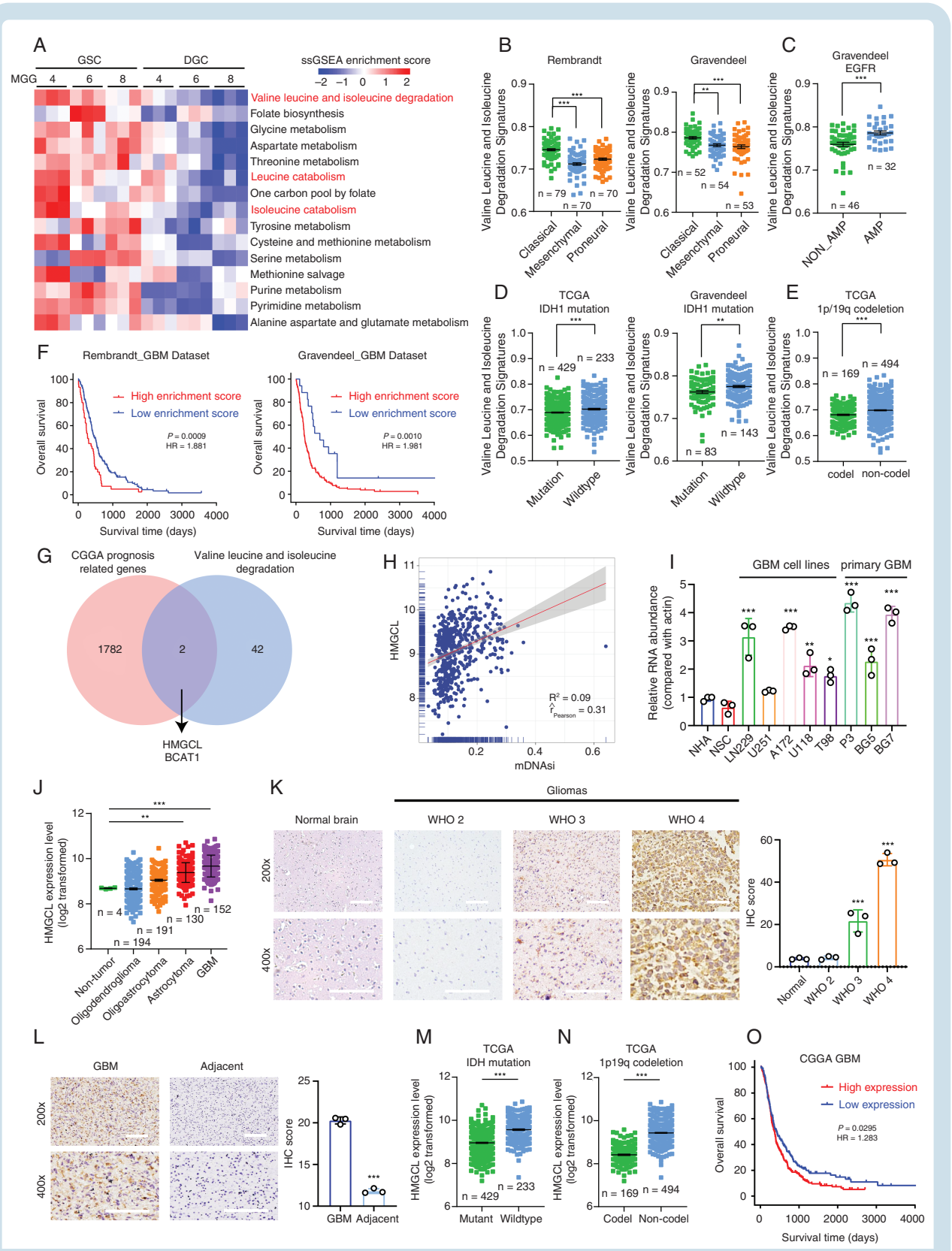

Figure 1. Branched-chain amino acid metabolism is essential for glioma stem cell (GSC) maintenance and glioblastoma multiforme (GBM) progression. (A) Single-sample GSEA of metabolic gene sets from the KEGG database in 3 GSCs (MGG4, MGG6, and MGG8) and matched differentiated GBM cells (DGCs). Each cell line contains 3 replicates from GSE54791. (B) Dot plots comparing valine, leucine, and isoleucine degradation activity

defined by corresponding gene set signatures in 3 GBM subtypes from Rembrandt and Gravendeel datasets. *n* indicates the number of biologically independent samples. Data are shown as the mean ± the standard error of the mean (SEM). ***$P < .001$; **$P < .01$. Statistical significance was determined with 1-way ANOVA. (C) Dot plots comparing GBM samples with or without *EGFR* amplification from the Gravendeel dataset. *n* indicates the number of biologically independent samples. Data are shown as the mean ± the standard error of the mean (SEM). ***$P < .001$. Statistical significance was determined with the 2-sided Student's *t* test. (D, E) Dot plots comparing all glioma samples with or without (D) *IDH1* mutation; (E) 1p/19q codeletion across data sets from GlioVis. *n* indicates the number of biologically independent samples. Data are shown as the mean ± the standard error of the mean (SEM). ***$P < .001$; **$P < .01$. Statistical significance was determined with the 2-sided Student's *t* test. (F) Kaplan–Meier plots of GBM patients grouped by valine, leucine, and isoleucine degradation signatures. (G) Venn plot displaying the valine, leucine, and isoleucine degradation gene set and independent prognosis-related genes from CGGA. (H) Correlation between HMGCL expression and mDNAsi score based on TCGA data sets. Statistical significance was determined with the *F* test. (I) qRT-PCR analysis of *HMGCL* mRNA expression in 2 noncancer cell lines, 5 GBM cell lines, and 3 primary GBM cell lines. Data are shown as the mean ± the standard error of the mean (SD). ***$P < .001$; **$P < .01$; *$P < .05$. Statistical significance was determined by 1-way ANOVA. (J) Dot plots comparing glioma samples based on histology from the TCGA data set. *n* indicates the number of biologically independent samples. Data are shown as the mean ± the standard error of the mean (SEM). ***$P < .001$; **$P < .01$. Statistical significance was determined with 1-way ANOVA. (K) Representative images of IHC staining of HMGCL in non-neoplastic brain ($n = 3$) and different pathological grades of gliomas ($n = 9$), and scoring. Scale bar = 100 μm. Data are shown as the mean ± the standard error of the mean (SD). ***$P < .001$. Statistical significance was determined with 1-way ANOVA. (L) Representative images of IHC staining for HMGCL in GBM and adjacent brain tissues from 3 paired samples, and scoring. Scale bar = 100 μm. Data are shown as the mean ± the standard error of the mean (SD). ***$P < .001$. Statistical significance was determined with the 2-sided Student's *t* test. (M) Dot plots comparing *HMGCL* expression in GBM samples with or without *IDH1* mutation across data sets from GlioVis. *n* indicates the number of biologically independent samples. Data are shown as the mean ± the standard error of the mean (SEM). ***$P < .001$. Statistical significance was determined with the 2-sided Student's *t* test. (N) Dot plots comparing *HMGCL* expression in GBM samples with or without 1p/19q codeletion across data sets from GlioVis. *n* indicates the number of biologically independent samples. Data are shown as the mean ± the standard error of the mean (SEM). ***$P < .001$. Statistical significance was determined with the 2-sided Student's *t* test. (O) Kaplan–Meier plots of GBM patients based on *HMGCL* high or low expression in tumors. A log-rank test was used to assess statistical significance.

(Threshold: $P < .001$) based on the CGGA database as described in a previous study[27] ($n = 1018$; Supplementary Table ST2). The analysis yielded 1784 genes related to prognosis. The intersection of this data set with the gene set of the valine, leucine, and isoleucine degradation genes yielded 2 genes, *BCAT1* and *HMGCL* (Figure 1G). While a tumor-promoting role for BCAT1 has been confirmed in GBM, function of HMGCL in GBM remains unknown. Thus, identifying the function for HMGCL and mediators of its function mechanism will contribute to a comprehensive understanding of BCAA metabolism in GBM progression. The mDNA-expression-based stemness index (mDNAsi) has been developed to examine the stemness of tumors as independent marker in TCGA glioma samples.[26] Our analysis demonstrated that *HMGCL* expression was positively correlated with the mDNAsi, further supporting a linkage with maintaining stemness of GSC (Figure 1H). Furthermore, *HMGCL* expression was higher in all GBM cell lines relative to neural stem cell (NSC) and normal human astrocytes (NHA), with the highest expression in primary GBM cell lines GBM#P3 and GBM#BG7 (Figure 1I). Therefore, increased HMGCL has a possible role in GSC maintenance and GBM progression.

The intratumoral expression pattern of *HMGCL* assessed with single-cell RNA-seq data[28] showed *HMGCL* was mainly expressed in malignant cells and to a lesser extent in oligodendrocyte and immune cells (Figure S1A). In addition, *HMGCL* expression was higher in GBM than in other gliomas, including astrocytoma, oligoastrocytoma, oligodendroglioma, and normal brain tissues, based on the TCGA data, further confirmed by the Rembrandt data (Figure 1J and Figure S1B). Increased expression of *HMGCL* was also detected in WHO 4 gliomas compared with lower-grade gliomas (Figure S1C and D).

To confirm that HMGCL protein levels were also increased in GBMs, we performed IHC staining for HMGCL on an independent cohort of glioma ($n = 9$) and normal brain tissue samples ($n = 3$). HMGCL protein levels were consistently higher in GBM compared with LGG and normal brain tissue samples. HMGCL was also localized to the cytoplasm (Figure 1K). IHC staining in a single GBM sample highlights these differences in HMGCL expression between tumor and adjacent brain (Figure 1L).

We subsequently assessed *HMGCL* levels based on molecular classifications of gliomas. Compared with *IDH1* mutated molecular subtype, the expression of *HMGCL* was higher in *IDH1* wild-type molecular subtype, crucial indicator for GBM according to 2021 WHO classification[1] (Figure 1M and Figure S1E). Furthermore, higher expression of *HMGCL* was observed in classical and mesenchymal GBM, relative to the other molecular subtypes based on the TCGA Verhaak-2017 molecular classification of GBM, associated with a poor prognosis (Figure S1F–H).

We next examined possible factors contributing to the differences in *HMGCL* expression between different molecular subtypes of gliomas. One critical feature of the *HMGCL* gene is that it resides on chromosome 1p36.11. Complete deletion of 1p/19q codeletion is molecular genetic hallmark of oligodendrogliomas, a subtype of low-grade glioma.[29] We found that LGGs and GBMs with 1p deletion had significantly lower *HMGCL* expression than nondeleted tumors in the data sets (Figure 1N, Figure S1I and J). Therefore, we examined the relationship between *HMGCL* copy number (CN) and expression. For both LGGs and GBMs, tumors with *HMGCL* heterozygous deletion (Hetloss) and homozygous deletion (Homdel) had significantly lower *HMGCL* mRNA expression than tumors that were diploid at 1p (Figure S1K). These results indicated that genetic and epigenetic alterations of *HMGCL* were associated with differences in *HMGCL* expression among gliomas.

To determine the clinical significance of high expression of *HMGCL*, Kaplan–Meier analysis was performed on

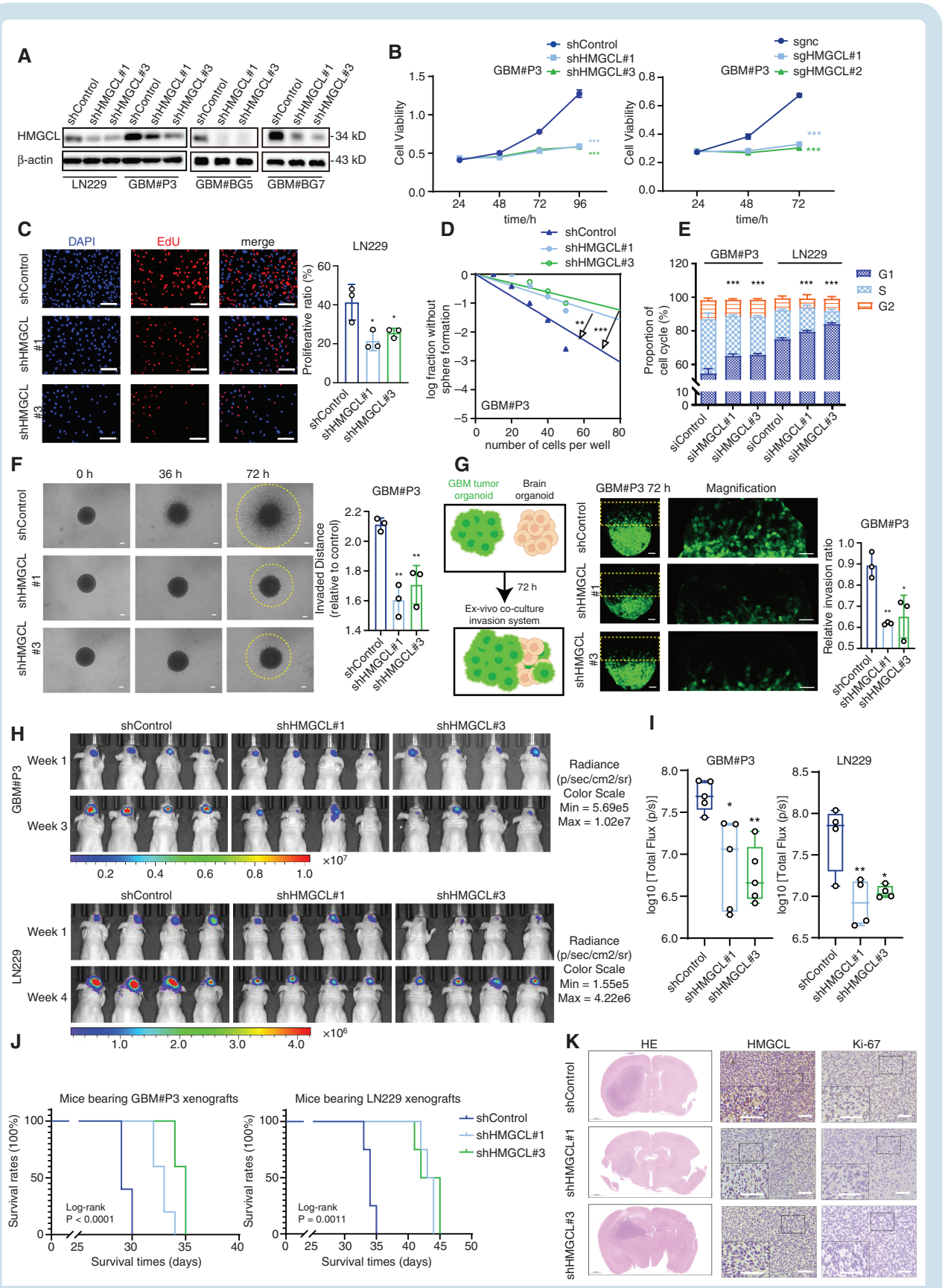

Figure 2. HMGCL knockdown inhibits glioblastoma multiforme (GBM) growth and glioma stem cell (GSC) maintenance in vitro and in vivo. (A) Western blot to detect HMGCL expression in LN229-, GBM#P3, GBM#BG5 and GBM#BG7-shControl, -shHMGCL#1, and -shHMGCL#3 cells (achieved with lentivirus). (B) CCK-8 assay for cell viability of HMGCL-knockdown/knockout GBM#P3. Shown are means and the SD ($n = 3$).

***P < .001. Statistical significance was determined with 2-way ANOVA. (C) EdU of LN229-shControl, -shHMGCL#1, and -shHMGCL#3. Scale bar = 100 μm. Shown are means and the SD (n = 3). *P < .05. Statistical significance was determined with the 2-sided Student's t test. (D) Extreme limiting dilution assays for GBM#P3-shControl, -shHMGCL#1, and -shHMGCL#3 cells to assess sphere formation. ***P < .001; **P < .01. Statistical significance was determined with pairwise tests. (E) Flow cytometry analysis of propidium iodide (PI) staining for the detection of the percentage of GBM#P3- and LN229 with transfection of siControl, siHMGCL#1, and siHMGCL#3 cells in different phases of the cell cycle. The percentage of cells arrested in the G1 phase is analyzed in bar graphs. Shown are means and the SD (n = 3). ***P < .001. Statistical significance was determined with 1-way ANOVA. (F) 3D tumor spheroid invasion assay to assess invasion of GBM#P3-shControl, -shHMGCL#1, and -shHMGCL#3. Scale bar = 100 μm. Shown are means and the SD (n = 3). **P < .01. Statistical significance was determined with 1-way ANOVA. (G) Model and representative images of coculture invasion assays for GBM#P3-shControl, -shHMGCL#1, and -shHMGCL#3 cells. Scale bar = 100 μm. Shown are means and the SD (n = 3). **P < .01; *P < .05. Statistical significance was determined with 1-way ANOVA. (H, I) Bioluminescence images and the corresponding quantification of tumors in mice implanted with GBM#P3- and LN229-shControl, -shHMGCL#1 and -shHMGCL#3 cells at week 1 (n = 5 per group), week 3 (for GBM#P3; n = 5 per group), and week 4 (for LN229; n = 4 per group). Shown are means and the SD. ***P < .001. Statistical significance was determined with 1-way ANOVA. (J) Kaplan–Meier survival curve of tumor-bearing mice implanted with GBM#P3- and LN229-shControl, -shHMGCL#1 and -shHMGCL#3 cells (n = 5 per group). A log-rank test was used to assess statistical significance. (K) Representative H&E staining and IHC for HMGCL and Ki-67 of orthotopic tumors derived from GBM#P3 cells. Scale bar = 100 μm.

survival of patients from databases. GBM patients with high *HMGCL* mRNA levels (based on best cutoff values) exhibited significantly better overall survival in all data sets (Figure 1O and Figure S1L–O).

Finally, univariate and multivariate COX analysis of *HMGCL* revealed expression of *HMGCL* as an independent prognostic indicator in glioma (Figure S1P and Q). Collectively, these results emphasized potentially prognostic relevance of *HMGCL* expression in GBM.

HMGCL Knockdown Inhibits GBM Growth and GSC Maintenance in Vitro and in Vivo

Next, we examined the role of HMGCL in the development of GBM in vitro. We knocked down HMGCL in the high-expressing cell lines LN229 and U251, and GSC line GBM#P3, GBM#BG5, and GBM#BG7 with lentiviral infection to generate cell populations stably expressing shRNAs (shControl, shHMGCL#1, and shHMGCL#3; Figure 2A; Figure S2A and B). HMGCL knockout cell lines were constructed by *CRISPR*/Cas9 (Figure S2C). GBM cell lines and GSCs expressing HMGCL-shRNAs showed reduced cell viability relative to controls (Figure 2B and Figure S2D). A similar tendency showed in HMGCL knockout cell lines (Figure 2B and Figure S2E). In contrast, knockdown of HMGCL did not alter cell viability of NHA (Figure S2F). Loss of HMGCL also led to reduced proliferation of LN229 and U251 cells in EdU assay (Figure 2C and Figure S2G). Furthermore, silencing HMGCL attenuated colony formation (Figure S2H and I) and self-renewal in GSCs (Figure 2D and Figure S2J–L), which was further confirmed in HMGCL knockout GBM#P3 (Figure S2M). Finally, flow cytometry demonstrated that the percentage of GBM#P3 and LN229 cells with transfection of siHMGCL in G1 phase increased. Therefore, loss of HMGCL may cause decreased cell proliferation by inducing cell cycle arrest in G1 (Figure 2E and Figure S2N).

We next assessed invasiveness of GBM cell lines in 3 in vitro assays. In Transwell assays, invasive ability was decreased in LN229- and U251-shHMGCL-1/-3 cells relative to controls (Figure S3A and B). In the 3D spheroid invasion assay, the proportion of spheres invading the Matrigel decreased ~30% relative to controls, also confirmed by HMGCL knockout cells (Figure 2F and Figure S3C and D). Finally, we used the coculture invasion model of tumor spheroids with healthy rat brain organoids as previously described to more accurately mimic the physiologically invasive tumor microenvironment.[30] GBM#P3-shHMGCL tumor spheres were less invasive into the rat brain organoids compared with control cell populations (Figure 2G).

To examine the effects of HMGCL loss on GBM growth in vivo, HMGCL-knockdown GBM#P3 and LN229 were implanted into mouse brains (4-week-old nude mice) to generate orthotopic xenografts. Tumor growth of P3- and LN229-shHMGCL-derived orthotopic xenografts was decreased relative to controls at weeks 3 and 4, respectively, while overall survival of tumor-bearing mice was increased (Figure 2H–J). IHC staining for the proliferation marker Ki-67 was reduced in P3-shHMGCL tumors, which was consistent with the inhibited tumor growth (Figure 2K and Figure S3E).

Taken together, the inhibition of HMGCL suppressed glioma proliferation in vitro and in vivo and self-renewal properties of GSC.

HMGCL-Mediated Alterations in Metabolism Cause Changes in Histone Acetylation Modification

As a rate-limiting enzyme in leucine metabolism and ketone body metabolism, HMGCL converts HMG-CoA into acetyl-CoA and acetoacetate. Acetoacetate is then converted into β-OHB by BDH1 or acetoacetyl-CoA by 3-oxoacid CoA-transferase 1 (OXCT1), and acetoacetyl-CoA is subsequently converted into acetyl-CoA by acetyl-CoA acetyltransferase 1 (ACAT1)[31] (Figure 3A). A previous study showed that production of β-OHB mediates HMGCL-induced tumorigenesis.[22] To determine the metabolite pathway underlying HMGCL-mediated metabolic change in GBM, we firstly investigated the expression of *BDH1*, *OXAT1,* and *ACAT1*. The expression of *ACAT1* was higher in GBM than normal brain samples, while expression of *BDH1* and *OXCT1* was decreased, indicating that conversion from acetoacetate to β-OHB might be blocked (Figure 3B). We therefore examined levels of the relevant metabolites in GBM cells with HMGCL knockdown. Knockdown of HMGCL led to a decrease in intracellular acetyl-CoA, but not β-OHB or acetoacetate (Figure 3C).

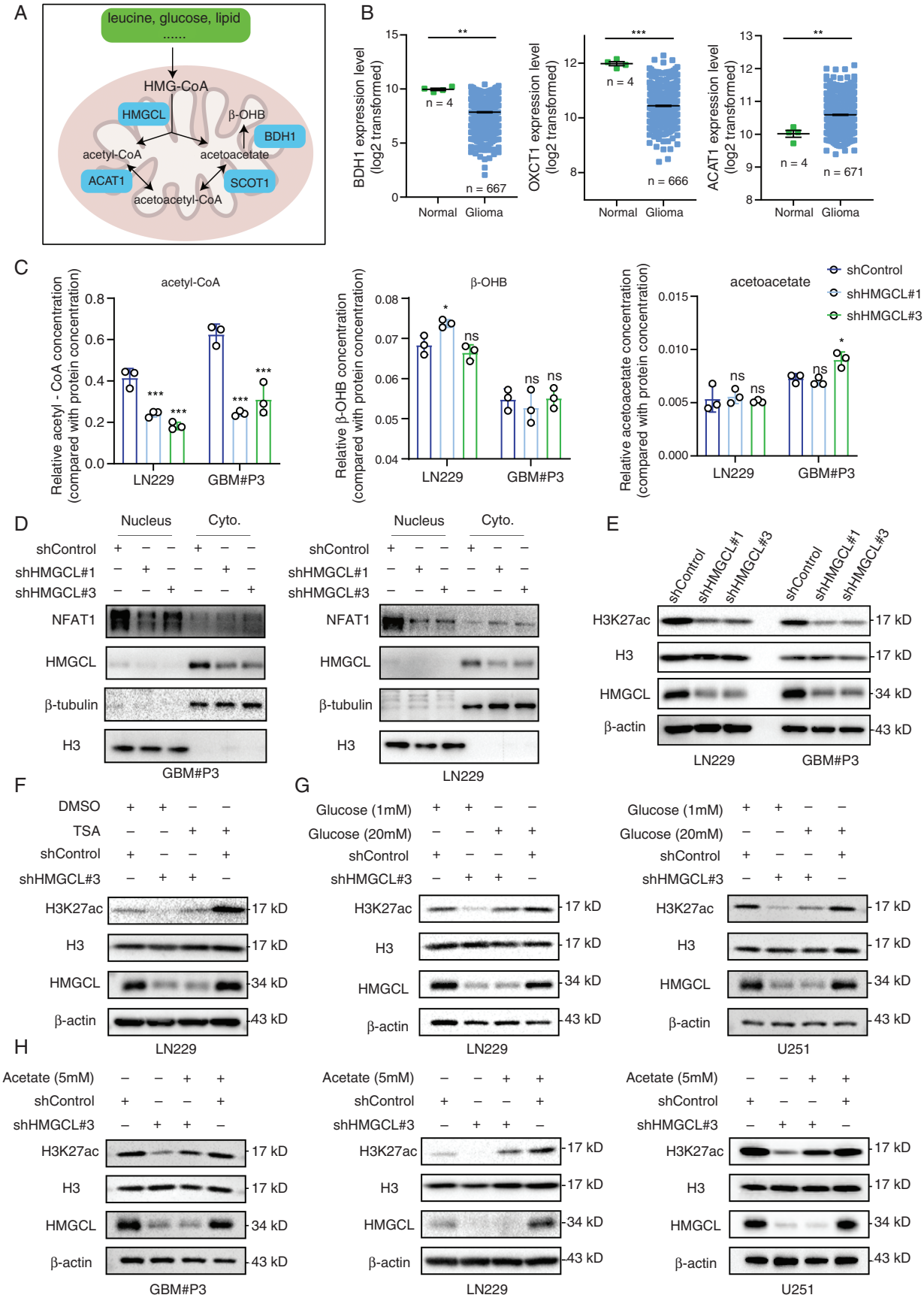

Figure 3. HMGCL-mediated alterations in metabolism caused histone acetylation modification change. (A) Schematic representation of HMGCL-mediated metabolic alteration. (B) *BDH1, ACAT1,* and *OXCT1* expression levels in tumors and normal brain tissues from the TCGA data set.

Shown are means and the SEM. ***$P < .001$; **$P < .01$. Statistical significance was determined with the 2-sided Student's *t* test. (C) Quantification of acetyl-CoA, β-OHB, and acetoacetate levels in GBM#P3-shControl, -shHMGCL#1, and -shHMGCL#3. Shown are means and the SD ($n = 3$). ***$P < .001$; *$P < .05$. Statistical significance was determined with 1-way ANOVA. (D) Western blot analysis to confirm NFAT1 subcellular location in LN229- and GBM#P3-shControl, -shHMGCL#1 and -shHMGCL#3. (E) Western blot analysis of H3K27ac modification of LN229- and GBM#P3-shControl, -shHMGCL#1 and -shHMGCL#3. (F) Western blot analysis of H3K27ac modification in LN229-shControl, -shHMGCL#1, and -shHMGCL#3 treated with or without TSA. (G) Western blot analysis of H3K27ac modification in LN229- and U251-shControl, -shHMGCL#1 and -shHMGCL#3 treated with variable concentrations of glucose. (H) Western blot analysis of H3K27ac modification in GBM#P3-, LN229- and U251-shControl, -shHMGCL#1 and -shHMGCL#3 treated with or without acetate.

As one of the main products of leucine degradation, acetyl-CoA functions not only as an intermediate metabolite for biosynthesis and catabolism processes, but also as a primary factor contributing to epigenetic modification, which is essential for GBM progression.[19,32] Histone acetylation promotes gene expression, which is potentially regulated by various metabolic activities and metabolic products.[33,34] Acetyl-CoA has been proposed to function as a donor in histone acetylation modification.[35] Indeed, intracellular acetyl-CoA abundance enhanced the global levels of histone acetylation and the expression of various genes linked to cell adhesion and migration.[12,35] Moreover, acetyl-CoA-mediated nuclear factor of activated T-cells (NFAT1) activation has been shown to contribute to site-specific modulation of histone acetylation, such as H3K27ac.[12] In LN229 and GBM#P3 cells, we found that nuclear accumulation of NFAT1 was inhibited after knockdown of HMGCL (Figure 3D and Figure S4A and B). Both glucose and acetate have been shown to serve as substrates for acetyl-CoA production.[32,36,37] Treatment with glucose and acetate could rescue nuclear NFAT1 level and showed no effect on total NFAT1 level, which supported our conclusion (Figure S4C–F). Overexpression of NFAT1 could also rescue inhibitory phenotypes of HMGCL knockdown cells (Figure S4G–I).

We therefore examined acetylation levels in histone 3 lysine 27 (H3K27) loci. Knockdown of HMGCL led to reduced levels of H3K27ac in LN229 and GBM#P3 cells (Figure 3E). We therefore treated cells with an inhibitor of histone deacetylase (HDAC), TSA. TSA rescued decreased H3K27ac levels in LN229 and GBM#P3 cells with loss of HMGCL (Figure 3F).

To further investigate whether HMGCL promoted acetyl-CoA-induced H3K27ac, we adjusted concentration of glucose and acetate in medium and examined the H3K27ac levels. In these experiments, elevated concentrations of glucose and acetate rescued decreased H3K27ac levels. Supplements with glucose and acetate could also rescue the inhibitory growth, self-renewal, and invasion with HMGCL knockdown (Figure 3G and H and Figure S5A–G).

Taken together, HMGCL-mediated elevation of acetyl-CoA promoted increased H3K27ac levels.

HMGCL Promotes *FOXM1* Expression and Regulates Cell Cycle Gene Expression

To further investigate the inhibiting effects of silencing HMGCL on cell proliferation and tumor growth, we performed transcriptome sequencing on U251-shHMGCL#3 and control to identify downstream targets potentially regulated by HMGCL-induced H3K27ac modification (Figure S6A). Analysis yielded a set of significant differentially expressed genes ($P < .05$ and $|\log2FC| > 0.6$). A heatmap was generated for the portion of genes downregulated in knockdown cells relative to controls ($P < .05$ and $\log2FC > 0.6$) (Figure 4A). We performed gene ontology (GO) enrichment analysis on differentially expressed genes ($P < .05$) with Metascape (https://metascape.org/) to identify putative pathways altered by HMGCL expression. GO analysis indicated that differentially expressed genes were closely related to biological processes involved in regulation of the cell cycle process and the mitotic cell cycle (Figure 4B).

To investigate key targets of HMGCL-mediated cell cycle changes, we considered intersection of significant differentially expressed genes ($P < .05$ and $|\log2FC| > 0.6$), "regulation of cell cycle process," "mitotic cell cycle" gene sets, and independent prognostic genes from CGGA data sets (Supplementary Table ST2 and Figure S6B). This analysis yielded *FOXM1* and *CASP2* as candidate gene targets for HMGCL-mediated cell cycle alterations (Figure 4C). As a transcription factor, Forkhead box protein M1 (FOXM1) exhibits a crucial role in the self-renewal and proliferation of stem cells, which also plays a role in the cell cycle regulation.[38–41] FOXM1 could regulate the expression of Wnt target genes by interaction with β-catenin in malignant gliomas and drive the ADAM17/EGFR activation loop to promote its mesenchymal transition.[41,42] In silico analysis showed that high expression of *FOXM1* in GBM and LGG compared to normal samples, which indicated a poor prognosis (Figure S6C and D). Expression of *FOXM1* was also higher in GSC than DGC (Figure S6E). Validation based on ChIP-seq data showed that H3K27ac peaks (marker of active promoters) within the promoter region of *FOXM1* were higher in GSCs and primary GBM samples than in DGCs (Figure S6F), indicating that high expression of *FOXM1* in GSCs may be induced by higher H3K27ac levels. However, *CASP2* has not been previously associated with glioma progression. Our results that HMGCL knockdown cell lines showed no significant alteration of *CASP2* confirmed this observation (Figure S6G). The above data supported the hypothesis that FOXM1 functioned as a key HMGCL downstream target involved in cell cycle regulation and glioma tumorigenesis.

Confirmation using qPCR analysis exhibited that mRNA expression of *FOXM1* was markedly reduced by HMGCL disruption in GBM#P3, LN229, and U251 cells (Figure 4D). Western blot analysis also confirmed that knockdown and knockout of HMGCL resulted in a reduction in FOXM1 protein levels (Figure 4E and Figure S7A). Finally, IHC

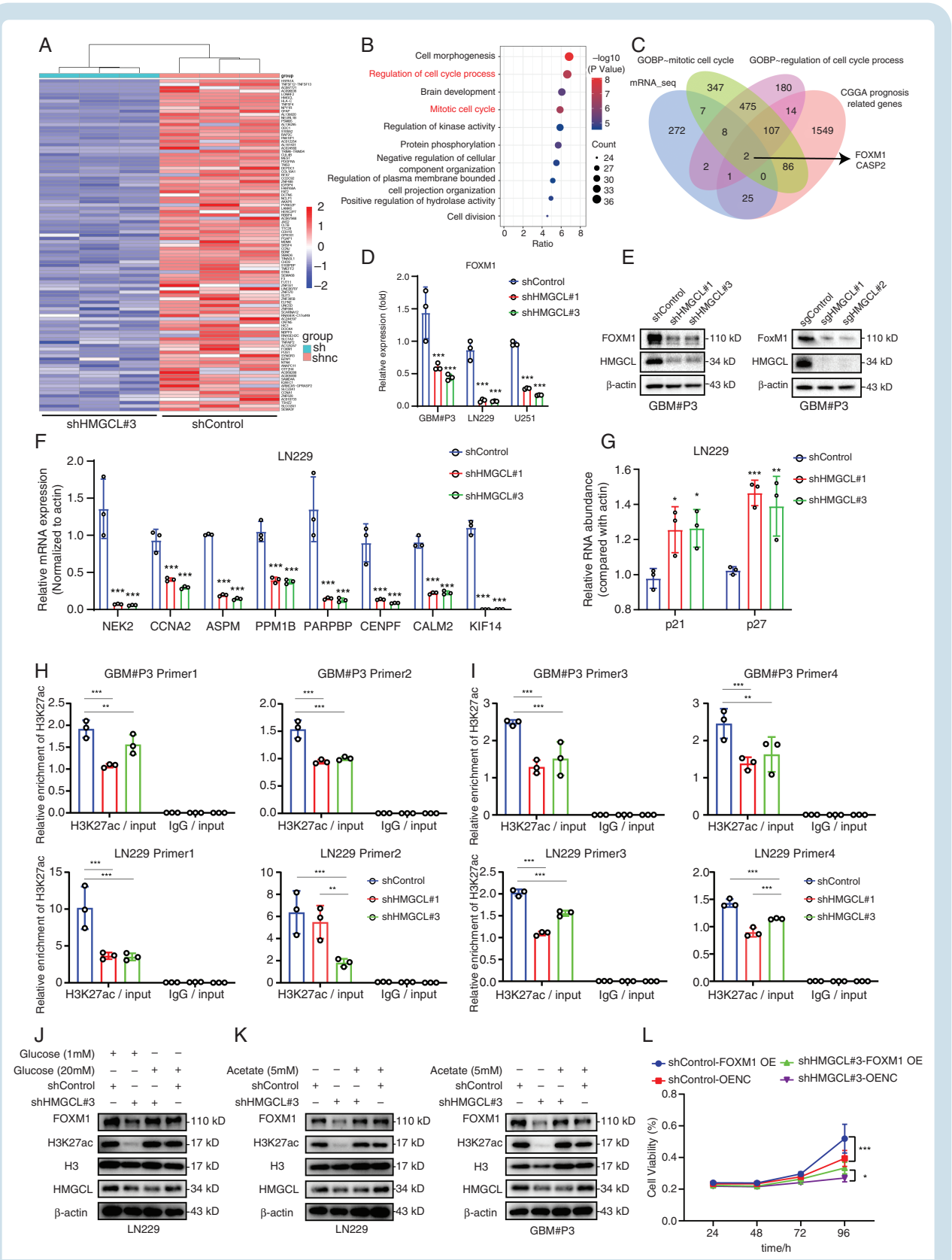

Figure 4. HMGCL promotes *FOXM1* expression and regulates cell cycle gene expression. (A) Heatmap of differentially expressed transcripts in RNA-seq data from U251 cells infected with shControl and shHMGCL-3 lentivirus. Gene expression data were mean *z*-transformed for display and colored red for high expression and blue for low expression. (B) GO enrichment analysis of differentially expressed genes based on RNA-seq data with *P* values. (C) Venn plot displaying the intersection of significantly downregulated mRNAs from the sequencing data, independent

prognosis-related genes, and specific gene sets. (D) qRT-PCR analysis of *FOXM1* in GBM#P3-, LN229- and U251-shControl, -shHMGCL#1 and -shHMGCL#3. *ACTB* was used as an internal control. Shown are means and the SD ($n = 3$). ***$P < .001$; **$P < .01$. Statistical significance was determined with 1-way ANOVA. (E) Western blot of FOXM1 in HMGCL knockdown/knockout GBM#P3. (F,G) qPCR analysis of FOXM1 downstream targets in LN229-shControl, -shHMGCL#1 and -shHMGCL#3 cells. Shown are means and the SD ($n = 3$). ***$P < .001$; **$P < .01$; *$P < .05$. Statistical significance was determined with 1-way ANOVA. (H,I) qPCR analysis of ChIP assays with the H3K27ac antibody or IgG GBM#P3- and LN229-shControl, -shHMGCL#1 and -shHMGCL#3. PCR primers amplified a fragment flanking the H3K27ac modified regions of *FOXM1* gene locus. Shown are means and the SD ($n = 3$). ***$P < .001$; **$P < .01$. Statistical significance was determined with 1-way ANOVA. (J) Western blot analysis of FOXM1 in LN229-shControl and -shHMGCL#3 LN229 treated with variable concentrations of glucose. (K) Western blot analysis of FOXM1 in LN229- and GBM#P3-shControl and -shHMGCL#3 treated with or without acetate. (L) CCK-8 assay for cell viability of LN229 -shControl and -shHMGCL#3 transfected with FOXM1-OE and empty vector. Shown are means and the SD ($n = 3$). ***$P < .001$; *$P < .05$. Statistical significance was determined with 2-way ANOVA.

staining of sections showed that FOXM1 protein levels were decreased in GBM#P3-shHMGCL#1- and GBM#P3-shHMGCL#3-derived xenografts compared with control samples (Figure S7B).

Analysis based on X2K Web (https://maayanlab.cloud/X2K/) revealed FOXM1 as a crucial transcription factor that induced transcription of other genes (Figure S7C). qPCR analysis demonstrated that knockdown of HMGCL decreased expression levels of FOXM1 transcriptional targets predicted by X2K (Figure 4F) as well as previously reported downstream genes[43] (Figure S7D). *CCNA2*, *CALM2*, and *CCNB2* have been confirmed to be involved in the cell cycle, while *ASPM*, *CENPF*, *PRC1*, *AURKB*, *TOP2A*, and *UBE2C* have been shown to be involved in mitosis. Disruption of HMGCL increased the expression of *p21* and *p27*, which are negatively regulated by FOXM1 (Figure 4G). This result indicated that reducing FOXM1 levels by HMGCL knockdown prohibited expression of cell cycle genes, consistent with cell cycle arrest.

In addition to transcriptional regulation, HMGCL may influence FOXM1 protein levels through posttranslational mechanisms. To determine whether HMGCL influenced FOXM1 protein stability, we treated HMGCL-knockdown cells with cycloheximide (CHX) (Figure S7E). The results showed that loss of HMGCL did not change the stability of FOXM1 protein.

Taken together, our results showed that FOXM1 was involved in regulating HMGCL-mediated cell cycle events in GBM cell lines.

HMGCL Promotes *FOXM1* Expression Through Promoter Acetylation

To determine molecular mechanism underlying HMGCL-induced expression of *FOXM1*, we examined promoter region of *FOXM1* through the UCSC genome database (http://www.genome.ucsc.edu/) for putative H3K27ac marks. Several H3K27ac marks were found in promoter region of *FOXM1* indicating possible transcriptional regulation of the gene dependent on H3K27ac modification. Thus, transcription of *FOXM1* might be regulated in part by HMGCL-mediated H3K27ac modification (Figure S8A).

To validate this hypothesis, we performed chromatin immunoprecipitation (ChIP) on lysates prepared from HMGCL-knockdown cells. Primers were designed based on H3K27ac modification region of *FOXM1* promoter. Lower levels of *FOXM1* fragments were captured by H3K27ac antibody-agarose complex in lysates from HMGCL-knockdown cells compared with controls. Binding of H3K27ac to the promoter region of *FOXM1* was attenuated after HMGCL silencing, demonstrating that HMGCL-regulated H3K27ac alteration influenced transcription of *FOXM1* (Figure 4H and I).

We next adjusted concentration of glucose and acetate in medium to determine whether either of these metabolites rescued H3K27ac modification levels and thus *FOXM1* expression. FOXM1 protein levels were rescued with higher concentrations of glucose (Figure 4J) or acetate (Figure 4K). Knockout of HMGCL inhibited H3K27ac modification and FOXM1 expression (Figure S8B). Further confirmation in GBM#BG5 and GBM#BG7 showed similar tendency (Figure S8C). The results further confirmed that alterations in *FOXM1* expression regulated by HMGCL were caused through changes in H3K27ac levels.

Notably, overexpression of *FOXM1* promoted tumor growth in LN229 or GBM#P3-shHMGCL#1/#3 cells. The result further confirmed a role for the HMGCL/FOXM1 axis in glioma growth (Figure 4L and Figure S8D).

To further support that these results were dependent on functional HMGCL, we transfected LN229 and GBM#P3 cells with a construct expressing an HMGCL mutant, HMGCL K48N. While overexpression of wild-type HMGCL increased H3K27ac and FOXM1 levels, overexpression of HMGCL K48N did not lead to changes in their protein levels (Figure S8E). However, overexpression of HMGCL weakly promoted or inhibited cell proliferation compared with negative control group and HMGCL K48N group (Figure S8F). The high expression of HMGCL in these GBM and GSC cell lines may accounted for this phenomenon (Figure 1I). Further confirmation by overexpressing HMGCL in HMGCL-knockdown cells showed rescue effect on inhibitory acetyl-CoA level, H3K27ac modification, FOXM1 expression, and GBM malignancies (Figure S9A–F). Overexpression of NFAT1 could also rescue inhibitory H3K27ac levels and FOXM1 level of HMGCL knockdown cells (Figure S9G).

In summary, these results indicated that HMGCL promotes transcription of *FOXM1* by enhancing H3K27ac modification.

HMGCL/FOXM1 Axis Promotes Nuclear Accumulation of β-Catenin

A key step in canonical Wnt signaling activation is nuclear translocation of β-catenin, which has been shown to be facilitated by its interaction with FOXM1 in glioma.[41] We

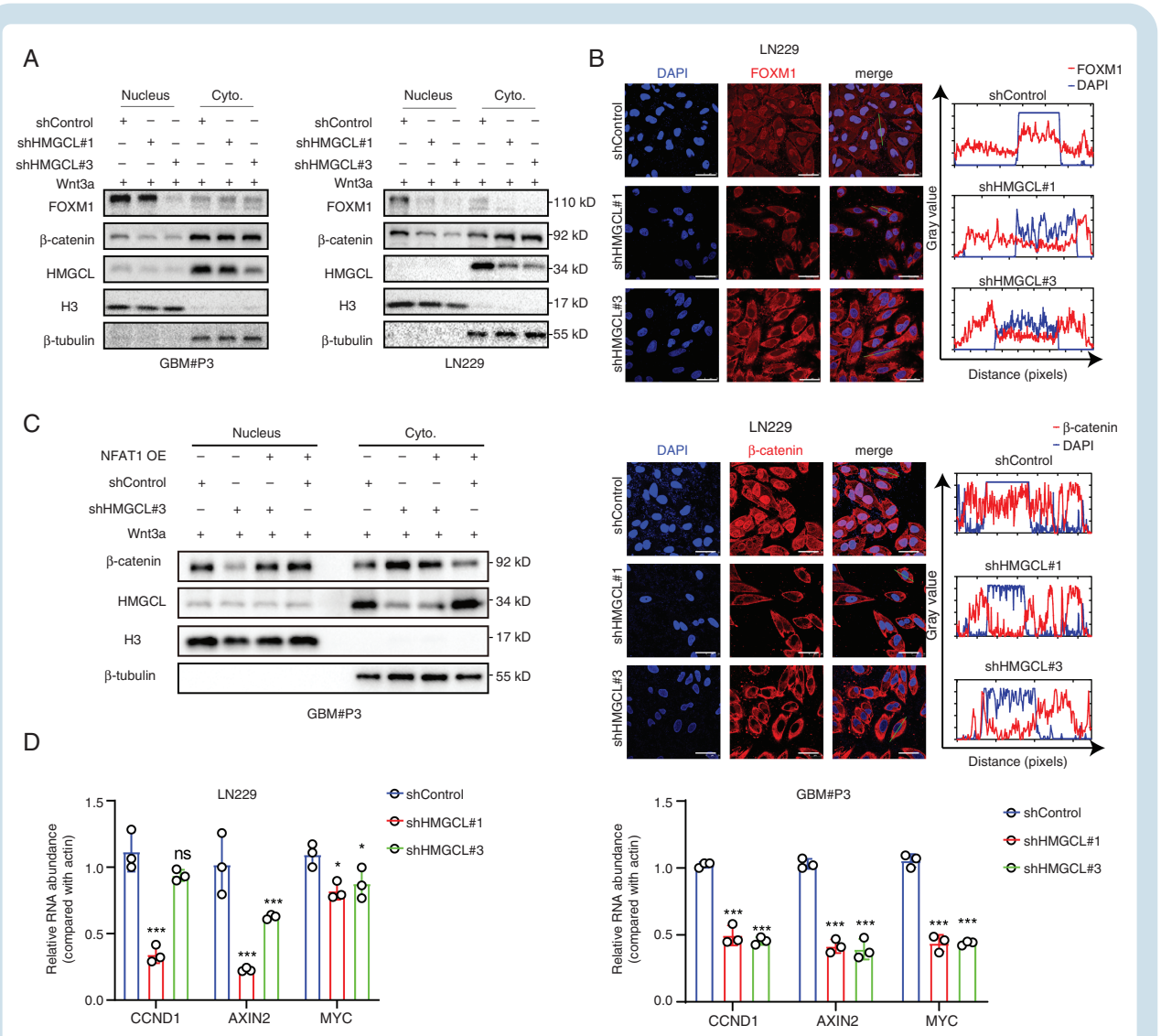

Figure 5. HMGCL/FOXM1 axis promotes nuclear accumulation of β-catenin. (A) Western blot for cytoplasmic and nuclear levels of FOXM1 and β-catenin in GBM#P3- and LN229-shControl, -shHMGCL#1 and -shHMGCL#3. The cells were treated with 20 ng/mL WNT3a for 60 minutes. (B) Double IF staining for FOXM1, β-catenin and DAPI in LN229-shControl, -shHMGCL#1 and -shHMGCL#3. The cells were treated with 20 ng/mL WNT3a for 60 minutes. Scale bar = 25 μm. (C) Western blot for cytoplasmic and nuclear levels of β-catenin with or without NFAT1 overexpression in GBM#P3-shControl and -shHMGCL#3 under treatment of 20 ng/mL WNT3a for 60 minutes. (D) qRT-PCR analysis of *CCND1*, *AXIN2* and *MYC* in LN229- and GBM#P3-shControl, -shHMGCL#1 and -shHMGCL#3. Shown are means and the SD ($n = 3$). ***$P < .001$; *$P < .05$; ns: $P > .05$. Statistical significance was determined with 1-way ANOVA.

therefore first asked whether HMGCL knockdown altered translocation of β-catenin by examining nuclear and cytoplasmic extracts prepared from HMGCL-knockdown cells and controls. Nuclear translocation of FOXM1 and β-catenin was attenuated after HMGCL silencing treated with WNT3a (Figure 5A). Immunofluorescence (IF) staining for β-catenin also showed a similar tendency for decreased nuclear translocation in HMGCL-knockdown cells (Figure 5B, Figure S10A and B). However, the mRNA levels of *CTNNB1* were not affected by HMGCL knockdown (Figure S10C). These results indicated that HMGCL influenced β-catenin expression at protein level. Increased nuclear β-catenin levels rescued by NFAT1 overexpression were confirmed in HMGCL knockdown cells (Figure 5C). Therefore, changes in FOXM1 expression mediated by HMGCL caused nuclear accumulation of β-catenin.

We next investigated expression levels of downstream targets of β-catenin with HMGCL knockdown. Downstream targets of β-catenin, including *CCND1*, *AXIN2*, and *MYC*, were all decreased in HMGCL-knockdown cells relative to controls. This result further demonstrated that transcriptional functions of β-catenin were inhibited in cells with HMGCL knockdown (Figure 5D).

In summary, the HMGCL/FOXM1 axis promoted nuclear accumulation of β-catenin, which is an essential protein involved in proliferation and invasion of GBM.

JIB-04 Interferes With the HMGCL/FOXM1 Axis and Is a Potential Molecular Agent for the Treatment of GBM

We next screened for potential drugs targeting HMGCL. The small molecule JIB-04 has been recognized as an inhibitor of histone demethylases (mainly KDM5A and KDM6B).[44] Previous work showed that JIB-04 was readily detectable in the brain of healthy mice with an intact BBB, which also induced cell cycle arrest and inhibition of cancer stem-like cell properties in hepatocellular carcinoma cells.[45] We therefore investigated whether JIB-04 inhibited the function of HMGCL in GBM cells.

Analysis performed with Autodock predicted that JIB-04 bound to HMGCL (Figure 6A and Figure S11A). Surface plasma resonance (SPR) exhibited a direct interaction between JIB-04 and HMGCL protein (Figure 6B). The result demonstrated that these 2 molecules interacted directly with each other.

To investigate the function of JIB-04 in GBM cell lines, we first determined the IC50 of JIB-04 for LN229 (0.1735 μM), U251 (0.2100 μM), NHA (6.552 μM), GBM#P3 (1.534 μM), GBM#BG5 (1.529 μM), and GBM#BG7 (1.930 μM) (Figure 6C). H3K27ac and FOXM1 levels gradually decreased with increasing JIB-04 concentration (Figure 6D and Figure S11B). Finally, histone methylation levels, especially for H3K4me3 and H3K27me3, showed no significant change when treated with the same doses of JIB-04 (Figure S11C).

Treatment with different concentrations of JIB-04 inhibited proliferation of LN229 and GBM#P3 cell lines, and inhibition of proliferation was JIB-04 dose-dependent (Figure 6E). Also, JIB-04 significantly reduced colony formation and self-renewal ability (Figure 6F–G and Figure S11D–H).

We also tested whether JIB-04 interfered with GBM cell invasion. In 3D invasion assays, JIB-04 significantly decreased invasion of GBM#P3 cells (Figure 6H). JIB-04 also reduced invasion of GBM#P3 and U251 cells into the rat brain organoids in the coculture invasion model (Figure 6I and Figure S11I).

Inhibitory effect of JIB-04 was also confirmed in vivo. GBM#P3 cells were orthotopically implanted in specific pathogen-free mice (4-week-old nude mice) and animals were injected i.p. with JIB-04 3 times each week. Tumor growth under treatment with JIB-04 was reduced compared with control (Figure 6J). The survival of GBM#P3 and LN229 tumor-bearing mice was also prolonged under JIB-04 treatment (Figure 6K). IHC staining for Ki-67 and FOXM1 were reduced in GBM#P3 tumors from animals treated with JIB-04 (Figure 6L and Figure S11J).

Toxicity of JIB-04 in normal tissues was evaluated in vitro and in vivo. Apoptotic ratio of NHA showed no significant alteration following GSC-treated doses of JIB-04 treatment (Figure S12A). Rat brain organoids treated with GSC-treated doses of JIB-04 showed no significant increase in the ratio of dead cells (Figure S12B). Histological evaluation of major organs in JIB-04-treated mice showed no abnormalities except for increased liver weights and liver vacuoles, which is consistent with research before[46] (Figure S12C).

Taken together, we demonstrated that JIB-04 interferes with the HMGCL/FOXM1 axis to inhibit GSC self-renewal and GBM progression.

Discussion

The importance and necessity of BCAA metabolic reprogramming in several types of human malignancies, including GBM, have recently been highlighted.[47] Despite their direct involvement in metabolic reprogramming processes, amino acids and their derivatives are also important for mediating epigenetic regulation.[13] In this present study, bioinformatic analysis showed that BCAA degradation was essential for GSC maintenance and GBM progression. Then *HMGCL*, a prognosis-related gene, was identified and investigated. *HMGCL* expression was found to be associated with WHO grade and malignant clinicopathological features of gliomas, whose elevated expression indicated a poor prognosis and functioned as an independent prognostic indicator. We used HMGCL knockdown as an innovative metabolic synthetic lethal approach to treat GBM and found that loss of HMGCL interfered with H3K27ac modification and decreased expression of FOXM1, which led to inactivation of β-catenin, a known oncogene in cancer development. Finally, targeting HMGCL with JIB-04 suppressed proliferation of tumor cells in vitro and in vivo. These results suggested that therapies targeting molecules in BCAA pathway may be developed for treatment of GBM.

In functional assays, we found that silencing of HMGCL suppressed GBM proliferation both in vitro and in vivo. HMGCL-mediated conversion from HMG-CoA to acetyl-CoA and acetoacetate. Previous studies showed that acetyl-CoA, partly generated from BCAAs, was required for histone acetylation processes that promote gene expression and cancer progression.[32] Acetyl-CoA has been shown to promote the upregulation of cell migration-related genes in GBM by controlling $Ca2^{+}$-NFAT signaling, which contributed to H3K27ac.[12] Our results also demonstrated that silencing HMGCL led to decreased acetyl-CoA levels and then promoted nuclear accumulation of NFAT1. Furthermore, acetylation levels at H3K27 might be regulated by silencing HMGCL, due to decreasing acetyl-CoA levels. However, since HMG-CoA is an important intermediate molecule located at the crossroads of leucine degradation and cholesterol biosynthesis mediated by HMGCR,[48] the level of cholesterol should also be investigated after interfering HMGCL. Acetyl-CoA, generated during leucine breakdown, is also utilized as a source for fueling TCA cycle for energy production. However, studies have revealed that there is no integration of BCAA carbon flow into TCA cycle intermediates in cancer cells.[19] Is this because current metabolic detection technologies have technical limitations? This pathway of metabolic intermediates must be investigated further in cancer cells. Since HMGCL is located at crossroads of ketone body production and BCAA degradation, deciphering its function should

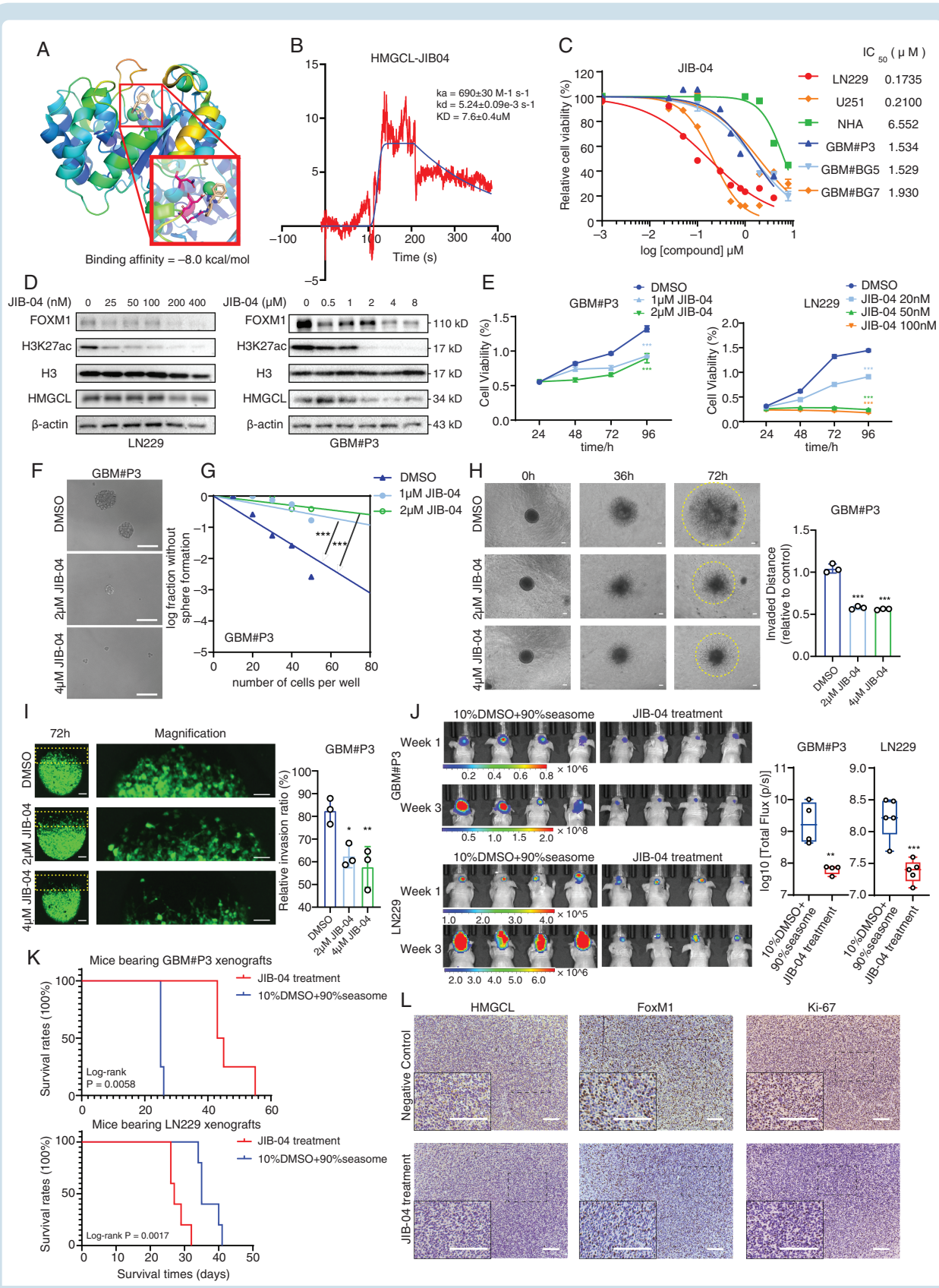

Figure 6. JIB-04 interferes with the HMGCL/FOXM1 axis and is a potential molecular agent for the treatment of Glioblastoma multiforme (GBM). (A) Surface mapping of JIB-04 (PubChem CID: 5825881) inside active site of HMGCL (PDB ID: 2CW6) with Autodock. (B) SPR assay showing global interaction of JIB-04 with HMGCL. Red line represents the raw data; and blue line is represents the line of best fit. (C) CCK-8 assay for relative cell viability of LN229, U251, NHA, GBM#P3, GBM#BG5 and GBM#BG7 treated with different concentrations of JIB-04 ($n = 3$) to generate

dose-inhibition curves and calculate IC50s. (D) Western blot to detect H3K27ac modification and FOXM1 in LN229 and GBM#P3 after treatment with different doses of JIB-04 and DMSO (vehicle control). (E) CCK-8 assay for relative cell viability of LN229 and GBM#P3 treated with JIB-04. Cell viability of the DMSO group was used for normalization. Shown are means and the SD ($n = 3$). ***$P < .001$. Statistical significance was determined with 2-way ANOVA. (F) Representative images of tumorsphere formation assays for GBM#P3 cells treated with JIB-04. Scale bar = 100 μm. (G) Extreme limiting dilution assays for GBM#P3 cells treated with JIB-04. Data are presented as the mean ± the SEM of 3 independent experiments. Statistical significance was determined with pairwise tests. (H) 3D tumor spheroid invasion assay to assess invasion of GBM#P3 treated with JIB-04. Scale bar = 100 μm. Shown are means and SD ($n = 3$). ***$P < .001$. Statistical significance was determined with 1-way ANOVA. (I) Model and representative images of coculture invasion assays for GBM#P3 treated with JIB-04. Scale bar = 100 μm. Shown are means and the SD ($n = 3$). **$P < .01$; *$P < .05$. Statistical significance was determined by 1-way ANOVA. (J) Bioluminescence images and the corresponding quantification of tumor volume in mice implanted with GBM#P3 and LN229 cells at day 7 ($n = 5$ per group), day 21 (for GBM#P3; $n = 4$ per group) and day 21 (for LN229; $n = 5$ per group). Shown are means and SD. ***$P < .001$; *$P < .05$. Statistical significance was determined with the 2-sided Student's *t* test. (K) Kaplan–Meier survival curve of GBM#P3 and LN220 tumor-bearing mice treated with JIB-04. (L) Representative images of IHC for HMGCL, FOXM1, and Ki-67 in the xenografts derived from GBM#P3. Scale bar = 100 μm.

be discussed in the light of metabolic and microenvironmental alterations. Alterations of metabolic processes and downstream targets brought by HMGCL are different in diverse tumor types. More researches are needed in order to get a comprehensive overview over its functions.

Previously recognized as a master regulator of the cell cycle, FOXM1 has multifaceted oncogenic potential as it is involved in invasion, self-renewal, and drug resistance.[49] Our experiments showed that alteration of H3K27ac induced by HMGCL promotes transcriptional of *FOXM1*. The influence of H3K27ac on expression of *FOXM1* was further confirmed in ChIP assays. However, with the development of epigenetics, posttranscriptional and posttranslational modifications have been identified that underlie the malignant transformation of normal cells into GBM. Acetylation of FOXM1 has been shown to influence its DNA binding affinity, protein stability, and phosphorylation sensitivity.[50] However, in our experiments, HMGCL knockdown failed to alter the stability of FOXM1 protein. With the development of research on protein and RNA acetylation modification, a comprehensive understanding of the epigenetic landscape of FOXM1 can be achieved.

JIB-04 was traditionally considered as a demethylation inhibitor and shown to inhibit the proliferation of temozolomide-resistant GBM cells.[44] Analysis performed with AutoDock predicted that JIB-04 interacted directly with HMGCL, confirmed by SPR. JIB-04 exerted an anticancer activity in GBM cells in vitro and in vivo. Also, it suppressed GBM through inhibition of H3K27ac and expression of FOXM1. Furthermore, at these concentrations, the methylation levels did not significantly change. Since HMGCL showed direct interaction with HMGCL and inhibit H3K27ac modification under suitable doses without methylation alteration, we consider it as a new mechanism, which is not in conflict with its classical effects. Analysis based on multiple targets contribute to its clinical use. However, specific mechanisms underlying the influence of JIB-04 on HMGCL function require further investigation.

In conclusion, our results demonstrated that HMGCL-mediated metabolic alteration and regulated H3K27 acetylation to promote *FOXM1* expression. Knockdown of HMGCL inhibited *FOXM1* expression levels and therefore its transcriptional activity as well as β-catenin nuclear accumulation. Moreover, JIB-04 exhibited anticancer activity in GBM cells by targeting the HMGCL/FOXM1 axis. These findings provide a novel therapeutic strategy for the treatment of GBM patients.

Supplementary Material

Supplementary material is available online at *Neuro-Oncology* (https://academic.oup.com/neuro-oncology).

Keywords

FOXM1 | glioblastoma | histone acetylation | HMGCL | metabolic regulation

Funding

This work was supported by the Natural Science Foundation of China (82103277), the Department of Science and Technology of Shandong Province (SYS202202, ZR2019ZD33, 2020CXGC010903, ZR2021QH030, and ZR2019PH042), the Research Project of Jinan Microecological Biomedicine Shandong Laboratory (JNL-2022003A, JNL-2022041C, and JNL-2022042C), the Clinical Research Center of Shandong University (2020SDUCRCB002), the Shandong Excellent Young Scientists Fund Program (2022HWYQ-035), the Special Foundation for Taishan Young Scholars (tsqn202211041), and the Qilu Young Scholar Program of Shandong University, China.

Conflict of Interest Statement

None declared.

Acknowledgments

The authors thank Prof. Rolf Bjerkvig and Prof. Hrvoje Miletic for establishing and providing primary GBM cells. The authors

would like to thank the CGGA, TCGA, Rembrandt, and Gravendeel networks for sharing the large data sets.

Data Availability

Data sets and other files generated, analyzed, or used during this study are available from the corresponding author upon reasonable request.

Authorship Statement

Y.S., X.Li., M.H., and B.H. designed this study and wrote the paper; Y.S., M.G., X.Z., and S.W. performed the experiments; Y.S., X.W., ZW.X., L.Z., and Y.G. analyzed the data; Y.W., F.Z., X.Liu., ZY.X., and Y.Z. collected patient samples. Y.S., C.W., J.L., W.L., S.N., and J.W. contribute to the revision work.

Affiliations

Department of Neurosurgery, Qilu Hospital, Cheeloo College of Medicine, Institute of Brain and Brain-Inspired Science, Shandong University, Jinan, China (Y.S., G.M., X.Z., Y.W., ZW.X., C.W., J.L., W.L., F.Z., X.Liu, ZY.X., Y.Z., S.N., J.W., X.Li, M.H., B.H.); Jinan Microecological Biomedicine Shandong Laboratory, Jinan, China (Y.S., X.Li, M.H., B.H.); Shandong Key Laboratory of Brain Function Remodeling, Jinan, China (Y.S., G.M., X.Z., Y.W., ZW.X., C.W., J.L., W.L., F.Z., X.Liu, ZY.X., Y.Z., S.N., J.W., X.Li, M.H., B.H.); Medical Integration and Practice Center, Cheeloo College of Medicine, Shandong University, Jinan, China (Y.S., G.M., ZW.X., M.H.); Department of Biomedicine, University of Bergen, Jonas Lies vei 91, 5009, Bergen, Norway (J.W.); Department of Neurosurgery, NYU Grossman School of Medicine, New York, New York, USA (S.W.); Department of Neurosurgery, Beijing Tiantan Hospital, Capital Medical University, Beijing, China (X.W.); Department of Clinical Laboratory, Qilu Hospital, Shandong University, Jinan, China (L.Z.); Department of Emergency Medicine, Chest Pain Center, Shandong Provincial Clinical Research Center for Emergency and Critical Care Medicine, Qilu Hospital, Shandong University, Jinan, Shandong, China (Y.G.)

References

1. Louis DN, Perry A, Wesseling P, et al. The 2021 WHO classification of tumors of the central nervous system: a summary. *Neuro Oncol.* 2021;23(8):1231–1251.
2. Wu W, Klockow JL, Zhang M, et al. Glioblastoma multiforme (GBM): an overview of current therapies and mechanisms of resistance. *Pharmacol Res.* 2021;171:105780.
3. Nicholson JG, Fine HA. Diffuse glioma heterogeneity and its therapeutic implications. *Cancer Discov.* 2021;11(3):575–590.
4. Hanahan D. Hallmarks of cancer: new dimensions. *Cancer Discov.* 2022;12(1):31–46.
5. Uddin MS, Mamun AA, Alghamdi BS, et al. Epigenetics of glioblastoma multiforme: from molecular mechanisms to therapeutic approaches. *Semin Cancer Biol.* 2022;83:100–120.
6. Tang L. Walking through chromatin modifications. *Nat Methods.* 2021;18(5):446.
7. Sese B, Ensenyat-Mendez M, Iniguez S, Llinas-Arias P, Marzese DM. Chromatin insulation dynamics in glioblastoma: challenges and future perspectives of precision oncology. *Clin Epigenetics.* 2021;13(1):150.
8. Amsalem Z, Arif T, Shteinfer-Kuzmine A, Chalifa-Caspi V, Shoshan-Barmatz V. The mitochondrial protein VDAC1 at the crossroads of cancer cell metabolism: the epigenetic link. *Cancers (Basel).* 2020;12(4):1031.
9. Etchegaray JP, Mostoslavsky R. Interplay between metabolism and epigenetics: a nuclear adaptation to environmental changes. *Mol Cell.* 2016;62(5):695–711.
10. Shteinfer-Kuzmine A, Verma A, Arif T, et al. Mitochondria and nucleus cross-talk: signaling in metabolism, apoptosis, and differentiation, and function in cancer. *IUBMB Life.* 2021;73(3):492–510.
11. Donohoe DR, Bultman SJ. Metaboloepigenetics: interrelationships between energy metabolism and epigenetic control of gene expression. *J Cell Physiol.* 2012;227(9):3169–3177.
12. Lee JV, Berry CT, Kim K, et al. Acetyl-CoA promotes glioblastoma cell adhesion and migration through Ca(2+)-NFAT signaling. *Genes Dev.* 2018;32(7-8):497–511.
13. Lieu EL, Nguyen T, Rhyne S, Kim J. Amino acids in cancer. *Exp Mol Med.* 2020;52(1):15–30.
14. Sivanand S, Vander Heiden MG. Emerging roles for branched-chain amino acid metabolism in cancer. *Cancer Cell.* 2020;37(2):147–156.
15. Zhang B, Chen Y, Shi X, et al. Regulation of branched-chain amino acid metabolism by hypoxia-inducible factor in glioblastoma. *Cell Mol Life Sci.* 2021;78(1):195–206.
16. Mayers JR, Torrence ME, Danai LV, et al. Tissue of origin dictates branched-chain amino acid metabolism in mutant Kras-driven cancers. *Science.* 2016;353(6304):1161–1165.
17. Weaver KJ, Holt RA, Henry E, Lyu Y, Pletcher SD. Effects of hunger on neuronal histone modifications slow aging in Drosophila. *Science.* 2023;380(6645):625–632.
18. Heng J, Wu Z, Tian M, et al. Excessive BCAA regulates fat metabolism partially through the modification of m(6)A RNA methylation in weanling piglets. *Nutr Metab (Lond).* 2020;17:10.
19. Peng H, Wang Y, Luo W. Multifaceted role of branched-chain amino acid metabolism in cancer. *Oncogene.* 2020;39(44):6747–6756.
20. Montgomery C, Pei Z, Watkins PA, Miziorko HM. Identification and characterization of an extramitochondrial human 3-hydroxy-3-methylglutaryl-CoA lyase. *J Biol Chem.* 2012;287(40):33227–33236.
21. Kang HB, Fan J, Lin R, et al. Metabolic rewiring by oncogenic BRAF V600E links ketogenesis pathway to BRAF-MEK1 signaling. *Mol Cell.* 2015;59(3):345–358.
22. Gouirand V, Gicquel T, Lien EC, et al. Ketogenic HMG-CoA lyase and its product beta-hydroxybutyrate promote pancreatic cancer progression. *EMBO J.* 2022;41(9):e110466.
23. Cui X, Yun X, Sun M, et al. HMGCL-induced beta-hydroxybutyrate production attenuates hepatocellular carcinoma via DPP4-mediated ferroptosis susceptibility. *Hepatol Int.* 2023;17(2):377–392.
24. Suva ML, Rheinbay E, Gillespie SM, et al. Reconstructing and reprogramming the tumor-propagating potential of glioblastoma stem-like cells. *Cell.* 2014;157(3):580–594.
25. Su A, Ling F, Vaganay C, et al. The folate cycle enzyme MTHFR is a critical regulator of cell response to MYC-targeting therapies. *Cancer Discov.* 2020;10(12):1894–1911.

26. Malta TM, Sokolov A, Gentles AJ, et al.; Cancer Genome Atlas Research Network. Machine learning identifies stemness features associated with oncogenic dedifferentiation. *Cell*. 2018;173(2):338–354.e15.
27. Liu W, Xu Z, Zhou J, et al. High Levels of HIST1H2BK in low-grade glioma predicts poor prognosis: a study using CGGA and TCGA Data. *Front Oncol*. 2020;10:627.
28. Neftel C, Laffy J, Filbin MG, et al. An integrative model of cellular states, plasticity, and genetics for glioblastoma. *Cell*. 2019;178(4):835–849.e21.
29. Ostrom QT, Bauchet L, Davis FG, et al. The epidemiology of glioma in adults: a "state of the science" review. *Neuro Oncol*. 2014;16(7):896–913.
30. Bjerkvig R, Laerum OD, Mella O. Glioma cell interactions with fetal rat brain aggregates in vitro and with brain tissue in vivo. *Cancer Res*. 1986;46(8):4071–4079.
31. Vallejo FA, Shah SS, de Cordoba N, et al. The contribution of ketone bodies to glycolytic inhibition for the treatment of adult and pediatric glioblastoma. *J Neurooncol*. 2020;147(2):317–326.
32. Pietrocola F, Galluzzi L, Bravo-San Pedro JM, Madeo F, Kroemer G. Acetyl coenzyme A: a central metabolite and second messenger. *Cell Metab*. 2015;21(6):805–821.
33. Sabari BR, Zhang D, Allis CD, Zhao Y. Metabolic regulation of gene expression through histone acylations. *Nat Rev Mol Cell Biol*. 2017;18(2):90–101.
34. Jo C, Park S, Oh S, et al. Histone acylation marks respond to metabolic perturbations and enable cellular adaptation. *Exp Mol Med*. 2020;52(12):2005–2019.
35. He W, Li Q, Li X. Acetyl-CoA regulates lipid metabolism and histone acetylation modification in cancer. *Biochim Biophys Acta Rev Cancer*. 2023;1878(1):188837.
36. Kamphorst JJ, Chung MK, Fan J, Rabinowitz JD. Quantitative analysis of acetyl-CoA production in hypoxic cancer cells reveals substantial contribution from acetate. *Cancer Metab*. 2014;2:23.
37. Wellen KE, Hatzivassiliou G, Sachdeva UM, et al. ATP-citrate lyase links cellular metabolism to histone acetylation. *Science*. 2009;324(5930):1076–1080.
38. Kalin TV, Ustiyan V, Kalinichenko VV. Multiple faces of FoxM1 transcription factor: lessons from transgenic mouse models. *Cell Cycle*. 2011;10(3):396–405.
39. Koo CY, Muir KW, Lam EW. FOXM1: from cancer initiation to progression and treatment. *Biochim Biophys Acta*. 2012;1819(1):28–37.
40. Wang Z, Park HJ, Carr JR, et al. FoxM1 in tumorigenicity of the neuroblastoma cells and renewal of the neural progenitors. *Cancer Res*. 2011;71(12):4292–4302.
41. Zhang N, Wei P, Gong A, et al. FoxM1 promotes beta-catenin nuclear localization and controls Wnt target-gene expression and glioma tumorigenesis. *Cancer Cell*. 2011;20(4):427–442.
42. Zhang C, Han X, Xu X, et al. FoxM1 drives ADAM17/EGFR activation loop to promote mesenchymal transition in glioblastoma. *Cell Death Dis*. 2018;9(5):469.
43. Tao W, Zhang A, Zhai K, et al. SATB2 drives glioblastoma growth by recruiting CBP to promote FOXM1 expression in glioma stem cells. *EMBO Mol Med*. 2020;12(12):e12291.
44. Romani M, Daga A, Forlani A, Pistillo MP, Banelli B. Targeting of histone demethylases KDM5A and KDM6B inhibits the proliferation of temozolomide-resistant glioblastoma cells. *Cancers (Basel)*. 2019;11(6):878.
45. Lee J, Kim JS, Cho HI, Jo SR, Jang YK. JIB-04, a pan-inhibitor of histone demethylases, targets histone-lysine-demethylase-dependent AKT pathway, leading to cell cycle arrest and inhibition of cancer stem-like cell properties in hepatocellular carcinoma cells. *Int J Mol Sci*. 2022;23(14):7657.
46. Wang L, Chang J, Varghese D, et al. A small molecule modulates Jumonji histone demethylase activity and selectively inhibits cancer growth. *Nat Commun*. 2013;4:2035.
47. Panosyan EH, Lin HJ, Koster J, Lasky JL, 3rd. In search of druggable targets for GBM amino acid metabolism. *BMC Cancer*. 2017; 17(1):162.
48. Luo J, Yang H, Song BL. Mechanisms and regulation of cholesterol homeostasis. *Nat Rev Mol Cell Biol*. 2020;21(4):225–245.
49. Kalathil D, John S, Nair AS. FOXM1 and cancer: faulty cellular signaling derails homeostasis. *Front Oncol*. 2020;10:626836.
50. Lv C, Zhao G, Sun X, et al. Acetylation of FOXM1 is essential for its transactivation and tumor growth stimulation. *Oncotarget*. 2016;7(37):60366–60382.